Top Catal (2016) 59:1110–1122
DOI 10.1007/s11244-016-0630-y

ORIGINAL PAPER

Effect of Coordination Environment in Grafted Single-Site Ti-SiO_2 Olefin Epoxidation Catalysis

Nicolás A. Grosso-Giordano[1] · Andrew Solovyov[1] · Sonjong Hwang[2] · Alexander Katz[1]

Published online: 10 June 2016

Abstract The effect of calixarene ligand symmetry, as dictated by lower-rim substitution pattern, on the coordination to a Ti(IV) cation is assessed in solution and when grafted on SiO_2, and its effect on epoxidation catalysis by Ti(IV)-calixarene grafted on SiO_2 is investigated. C_{2v} symmetric Ti-*tert*-butylcalix[4]arene complexes that are 1,3-alkyl disubstituted at the lower rim (di-R-Ti) are compared to previously reported grafted C_s symmetric complexes, which are singly substituted at the lower rim (mono-R-Ti). ^{13}C MAS NMR spectra of complexes isotopically enriched at the lower-rim alkyl position indicate that di-R-Ti predominantly grafts onto silica as the conformation found in solution, exhibiting a deshielded alkyl resonance compared to the grafted mono-R-Ti complexes, which is consistent with stronger alkyl ether→Ti dative interactions that are hypothesized to result in higher electron density at the Ti center. Moreover, ^{13}C MAS NMR spectroscopy detects an additional contribution from an "endo" conformer for grafted di-R-Ti sites, which is not observed in solution. Based on prior molecular modeling studies and on ^{13}C MAS NMR spectroscopy chemical shifts, this "endo" conformer is proposed to have similar Ti–(alkyl ether) distances at the lower-rim and electron density at the Ti center relative to grafted mono-R-Ti complexes. Differences between grafted mono-R-Ti and di-R-Ti sites can be observed by ligand-to-metal charge transfer edge-energies, calculated from diffuse-reflectance UV–visible spectroscopy at 2.24 ± 0.02 and 2.16 ± 0.02 eV, respectively. However, rates of *tert*-butyl hydroperoxide consumption in the epoxidation of 1-octene are found to be largely unchanged when compared to those of the grafted mono-R-Ti complexes, with average rate constants of ~ 1.5 M^{-2} s^{-1} and initial TOF of ~ 4 ks^{-1} at 323 K. This suggests that an "endo" conformation of grafted di-R-Ti may prevail during catalysis. Despite this, grafted di-C_1-Ti complexes can be more selective than mono-C_1-Ti complexes (45 vs. 34 % at a 50 % conversion at 338 and 353 K), illustrating the importance of the Ti coordination environment on epoxidation catalysis.

Keywords Terminal olefin epoxidation · Titanium calixarene · Organic hydroperoxide · Tert-butyl hydroperoxide · Heterogeneous catalysis · Coordination environment · Ligand-to-metal charge-transfer · Grafted organometallic complex conformation

1 Introduction

Heterogeneous catalysts often present non-uniform active surfaces which are difficult to characterize at the molecular level. The understanding of structure–function relationships in heterogeneous catalysts continues to be a challenging and rewarding pursuit, since these relationships enable catalyst optimization in a way that is rooted in rational molecular-level design, at the state of the art of the field. This understanding benefits from being able to precisely control the synthesis of uniform catalytic active

Electronic supplementary material The online version of this article (doi:10.1007/s11244-016-0630-y) contains supplementary material, which is available to authorized users.

✉ Alexander Katz
askatz@berkeley.edu

[1] Department of Chemical and Biomolecular Engineering, University of California at Berkeley, Berkeley, CA 94720, USA

[2] Division of Chemistry and Chemical Engineering, California Institute of Technology, Pasadena, CA 91125, USA

sites, such that specific molecular features can be correlated to catalytic performance [1], and in a way that leverages on characterization of soluble catalyst precursors in solution [2–4].

Ti(IV) on silica is a well known active and selective Lewis acid catalyst for olefin epoxidation, particularly when found as isolated, tetrahedrally coordinated active sites embedded or grafted on a heterogeneous support [5–7]. Indeed, titanosilicates represent a class of materials broadly used in epoxidation but only understood at the atomic level in a limited way [3, 8–13], . For example, while there is agreement that six-coordinate, coordinatively saturated Ti sites, as found in bulk TiO_2, are inactive, it remains unobvious whether the ideal site for catalysis is an isolated Ti or slightly oligomeric species with Ti–O–Ti connectivity [14].

Our research group has pioneered the use of grafted metallocalixarene [15] complexes as a strategy to synthesize isolated Ti active sites with controllable molecular environments, which maintain site isolation and provide a precise model system to study heterogeneous catalysts [16–19]. Using titanocalixarene model systems, we correlated 3d-orbital occupancy at grafted Ti centers on SiO_2 to Lewis acidity and catalytic activity [17] for olefin epoxidation using an organic hydroperoxide as the oxidant. This was a demonstration that the connectivity and coordination of a Ti center, as enforced by an organic ligand, could be synthetically tailored to control the molecular environment of a working catalyst active site on a surface.

The strong difference between the two titanocalixarene complexes used in this prior study [17], however, led us to look for opportunities to alter Ti coordination in subtler ways; therefore, we continue our studies here, with calixarene ligands where only differences in dative interactions to Ti are possible. Based on studies of vanadocalixarenes, we hypothesized that the lower-rim symmetry of *p-tert*-butylcalix[4] arene complexes should influence dative interactions and 3d occupancy at the Ti center, and thus could have a measurable impact on catalytic activity [20]. In particular, we hypothesized that C_{2v} symmetric calixarene ligands (di-R in Scheme 1) should impart a higher 3d-orbital electron density on the Ti center than C_s symmetric ligands (mono-R in Scheme 1), based on the shorter alkoxy ether oxygen–titanium dative distances in di-R relative to mono-R complexes. We thus predicted depressed epoxidation rates for Ti complexes of the di-R ligand.

In this work, we tested this hypothesis by synthesizing four titanocalixarene complexes, consisting of two different symmetries controlled by different lower-rim substituents, which we immobilized onto dehydroxylated silica supports. These catalysts were tested for the epoxidation of 1-octene using *tert*-butyl hydroperoxide (TBHP), an oxidant widely used in the industrial epoxidation of olefins [21]. Catalytic activity and selectivity were used to investigate the influence of coordination environment on catalysis. The main difference between the synthesized titanocalixarenes was dictated by ligand coordination of mono-R versus di-R ligands (see Scheme 1, where R = alkyl chain). Mono-C_1-Ti has been previously synthesized, characterized [22], grafted, and studied for alkene epoxidation [15–17]; it is stable when grafted, has C_s symmetry, displays one weak methoxy oxygen–Ti dative interaction, and is an active epoxidation catalyst. The di-C_1-Ti complex has been synthesized [23, 24], but to our knowledge it has never been grafted on a surface or tested in olefin epoxidation. It is stable at room temperature, has C_{2v} symmetry, and displays two stronger methoxy oxygen–Ti interactions as a result of shorter RO–Ti distances. Analogous mono-C_5 and di-C_5, with pentoxy replacing methoxy alkyl ether substituents were also synthesized to investigate lower-rim substituent effects. These four ligands were used to synthesize metallocalixarenes complexes, which were grafted onto SiO_2 resulting in active epoxidation catalysts with varying inner-sphere coordination environments. In addition, outer-sphere effects were studied by varying the hydroxyl density of the SiO_2 support surface by pre-treating SiO_2 at different temperatures.

We first describe the synthesis of grafted titanocalixarene materials and confirm the intact grafting of complexes onto SiO_2 by a combination of elemental analysis and solid-state ^{13}C NMR spectroscopy. Using calixarene ligands isotopically enriched at the methoxy position (O–R positions in Scheme 1) and ^{13}C MAS NMR spectroscopy, we demonstrate that di-C_1-Ti grafts in two different conformations, consistent with previously published molecular modeling results of solution-phase conformations of Ti-calixarene complexes [24]. Diffuse reflectance UV–visible spectroscopy is used as a probe for measuring ligand-to-metal-charge-transfer (LMCT) edge energies in complexes with different symmetries. We then use these materials to investigate the postulated hypothesis on the influence that dative interactions to Ti have on catalytic performance in olefin epoxidation, when using TBHP as oxidant.

2 Experimental

2.1 General Experimental

Tert-Butylcalix[4] arene was purchased from Aldrich. Chemical reagents were purchased at reagent grade quality and were used without further purification unless otherwise noted. Toluene was freshly distilled over sodium/

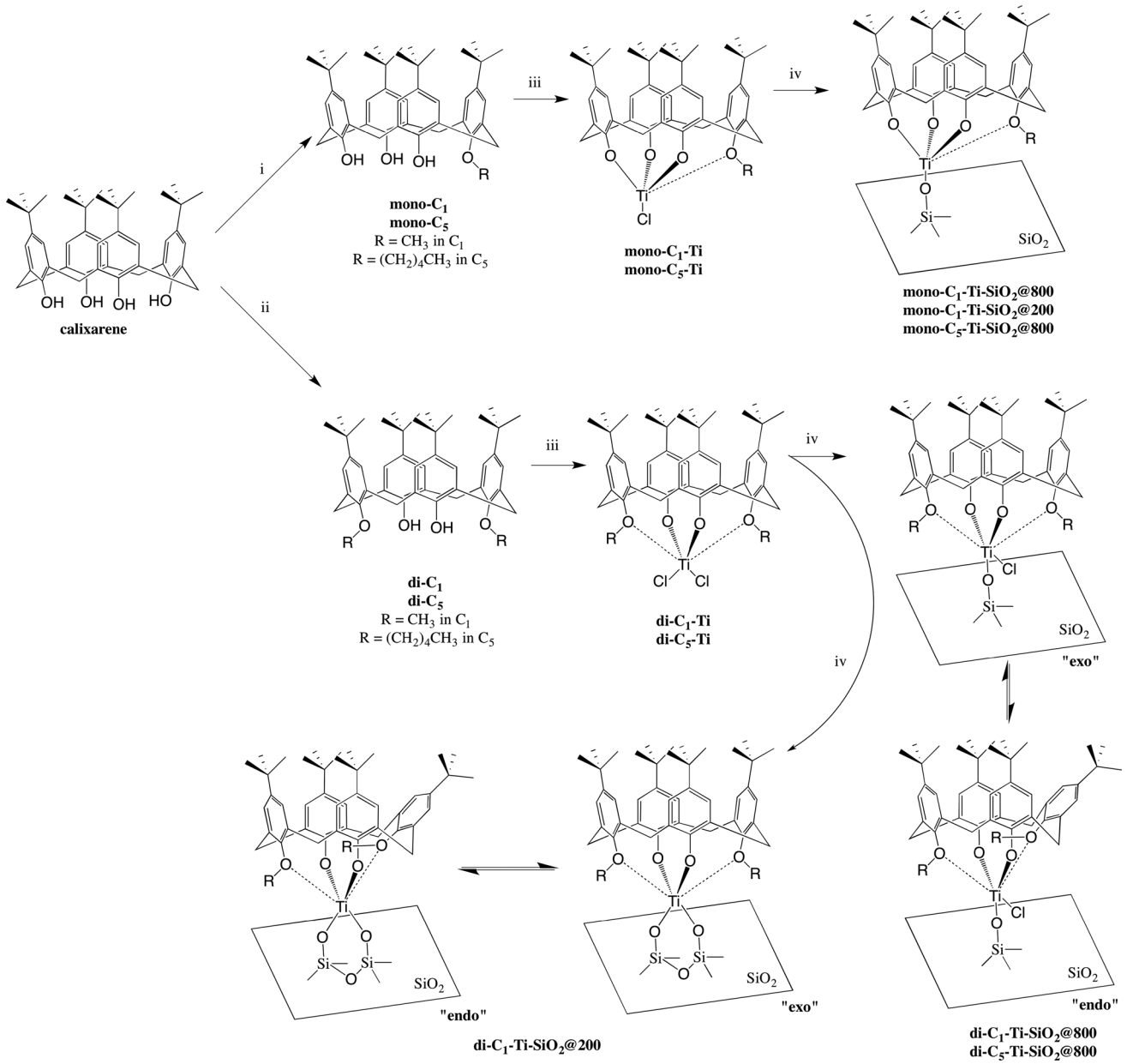

Scheme 1 Synthesis of Grafted Calixarene-Ti Materials. (i) 1.1 equiv CsF, 2 equiv of iodomethane or 1-bromopentane, DMF, 333 K 18 h; (ii) 3 equiv K_2CO_3, 3 equiv iodomethane or 1-brompentane, DMF, 333 K 48 h; (iii) 0.9 equiv $TiCl_4$, anhydrous toluene, 313 K, 1.5 h; (iv) SiO_2 surface, toluene, ambient temperature, 24 h. O-Ti dative interactions are shown in with dashed lines. di-C_1-Ti-SiO_2@800, di-C_5-Ti-SiO_2@800, di-C_1-Ti-SiO_2@200 are hypothesized structures. *Reversible arrows* indicate the two proposed conformations for the complex on the surface

benzophenone. Benzene-d6 was distilled over sodium and stored over pretreated molecular sieves. DMF was used as received. Reactions were monitored with TLC on Selecto 60 plates. Silica gel chromatography purification of calixarene ligands was performed using Selecto 60 silica gel (0.32–0.64 mm particle size). Synthesis of titanocalixarenes was performed under Ar using Schlenk techniques. $TiCl_4$ was used as 1.0 M solution in toluene (Aldrich).

2.2 General Analytical

Carbon–hydrogen–nitrogen analysis was performed at UC Berkeley Microanalytical facility using a Perkin Elmer 2400 Series II combustion analyzer, and grafted calixarene loadings were estimated by assuming that carbon contents were entirely due to the presence of calixarenes mono-C_1, mono-C_5, di-C_1, and di-C_5. Ti contents were measured by ICP-AES

at Galbraith Laboratories. Cl contents were measured by suppressed ion chromatography at Galbraith Laboratories.

Support surface areas were determined by the BET method from N_2 physisorption measurements performed with a Micromeritics ASAP 2020 instrument at 77 K after sample evacuation at 623 K for 4 h.

Diffuse reflectance UV–visible spectra were measured at ambient conditions using a Varian Cary 4000 Specrophotometer fitted with a Praying Mantis attachment from Harrick Scientific Instruments. Compacted poly-(tetrafluroethylene) powder was used as a perfect reflector standard for baseline corrections, and all spectra are reported using Kublka–Munk pseudo-absorbance. LMCT edge energies of the materials were calculated following methods previously used for titanocalixarenes [16]. Slopes of tangent lines as shown in Fig. 3 were calculated from the first derivative of the transformed spectra, and were drawn tangent to the spectra at their point of inflection.

Solid-state ^{13}C magic-angle spinning (MAS) NMR signals were collected using a Bruker DSX-500 spectrometer and a Bruker 4 mm MAS probe at the Caltech Solid-State NMR Facility. Solution NMR spectra were measured using a Bruker AM-400 spectrometer at the UC-Berkeley NMR Facility. ES mass spectra were recorded at the UC Berkeley Mass Spectrometry Facility.

2.3 Calixarene Ligand, Titanocalixarene, and Grafted Material Synthesis

Synthesis of ligand, titanocalixarene complexes, and grafted materials are summarized in Scheme 1.

2.3.1 Calixarene Ligands

Regioselective functionalization of calixarenes is well known [25]. Using a weak base in alkylation of calixarenes affords distal-1,3-dialkylated product with good yield [26]. By reaction of *tert*-butyl-calix[4]arene with three equivalents of potassium carbonate and excess haloalkane, we synthesized distal dialkylated calixarene with good yield. For the selective synthesis of monoalkyl-calixarene, a protection-deprotection strategy [27], using a weaker base like cesium fluoride [28], or lower loadings of potassium carbonate and reaction condition variation have been reported [29]. In our study, we used a direct monoalkylation method based on reaction of *tert*-butyl-calix[4]arene with 1:1 equavelent of cesium fluoride with moderate yields.

2.3.1.1 General Procedure for Synthesis of mono-C_1, mono-C_5 To a mixture of *tert*-butylcalix[4]arene (2.88 mmol) and CsF (3.17 mmol) in 30 ml of dry DMF, methyl iodide or 1-bromopentane (5.76 mmol) was added at 40 °C. The resulting mixture was heated at 50 °C for 18 h. The solvent was evaporated and the residue was re-dissolved in chloroform. This solution was washed with water, and the organic layer was dried over sodium sulfate and evaporated to dryness. The white product was purified using column chromatography.

5,11,17,23-tetra-*tert*-butyl-25-(^{13}C-methoxy)-26,27,28-trihydroxy-calix[4] arene (mono-C_1). After purification via column chromatography (eluent DCM/n-hexane 1:1 v/v, R_f 0.9), a white powder was obtained in 43 % yield; ^{1}H NMR ($CDCl_3$): δ 10.20 (s, 1H, O*H*), 9.60 (s, 2H, O*H*), 7.13 (m, 2H, Ar*H*), 7.09 (d, 2H, $^4J = 2.0$ Hz, Ar*H*), 7.08 (s, 2H, Ar*H*), 7.02 (d, 2H, $^4J = 2.0$ Hz, Ar*H*), 4.39 (d, 2H, $^2J = 12.5$ Hz, ArCH_2Ar), 4.30 (d, 2H, $^2J = 12.5$ Hz, ArCH_2Ar), 4.16 (d, 3H, $^1J = 144.9$ Hz, $^{13}CH_3$), 3.47 (d, 4H, $^2J = 14.0$ Hz, ArCH_2Ar), 1.26 (s, 9H, t-C$_4H_9$), 1.24 (s, 18H, t-C$_4H_9$), 1.23 (s, 9H, t-C$_4H_9$); ^{13}C NMR($CDCl_3$): δ 148.32, 147.83, 143.61, 143.22, 133.43, 128.20, 127.90, 126.51, 125.80, 125.73, 125.69, 63.28, 34.28, 34.03, 33.96, 33.02, 32.12, 31.51, 31.28; HR ESI MS calcd for $^{12}C_{44}^{13}C_1H_{57}O_4$ 662.4296, found 662.4280.

5,11,17,23-tetra-*tert*-butyl-25-(1-pentyloxy)-26,27,28-trihydroxy-calix [4] arene (mono-C_5). After purification via column chromatography (eluent DCM/n-hexane 1:1 v/v, R_f 1.0), a white powder was obtained in 49 % yield; ^{1}H NMR ($CDCl_3$): δ 10.29 (s, 1H, O*H*), 9.69 (s, 2H, O*H*), 7.17 (s, 2H, Ar*H*), 7.14 (d, 2H, $^4J = 2.4$ Hz, Ar*H*), 7.13 (s, 2H, Ar*H*), 7.06 (d, 2H, $^4J = 2.4$ Hz, Ar*H*), 4.44 (d, 2H, $^2J = 12.8$ Hz, ArCH_2Ar), 4.36 (d, 2H, $^2J = 13.6$ Hz, ArCH_2Ar), 4.21 (t, 2H, $^3J = 7.2$ Hz, OCH_2), 3.52 (d, $^2J = 13.6$ Hz, ArCH_2Ar), 3.50 (d, $^2J = 12.8$ Hz, ArCH_2-Ar), 2.24 (m, 2H, CH_2), 1.69 (m, 2H, CH_2), 1.60 (m, 2H, CH_2), 1.30 (s, 9H, t-C$_4H_9$), 1.29 (s, 18H, t-C$_4H_9$), 1.27 (s, 9H, t-C$_4H_9$), 1.08 (t, 3H, $^3J = 7.2$ Hz, CH_3); ^{13}C NMR($CDCl_3$): δ 149.47, 148.54, 148.07, 147.87, 143.63, 143.12, 133.58, 128.40, 128.22, 127.73, 126.44, 125.99, 125.78, 125.75, 125.69, 76.76, 34.28, 34.06, 33.97, 33.08, 32.31, 31.56, 31.54, 31.47, 31.32, 29.53, 28.05, 22.59, 14.15; HR ESI MS calcd for $^{12}C_{49}H_{65}O_4$ 717.4888, found 717.4872.

2.3.1.2 General Procedure for Synthesis of di-C_1, di-C_5 To a mixture of *tert*-butylcalix[4]arene (1.54 mmol) and potassium carbonate (4.60 mmol) in 25 ml of dry DMF, methyl iodide or 1-bromopentane (4.60 mmol) was added at 40 °C. The resulting mixture was heated at 50 °C for 48 h. The solvent was evaporated and the residue was re-dissolved in chloroform. This solution was washed with water, and the organic layer was dried over sodium sulfate and evaporated to dryness. The white product was purified using column chromatography.

5,11,17,23-tetra-*tert*-butyl-25, 27(di-^{13}C-methoxy)-26, 28-dihydroxy-calix[4]arene (di-C_1). After purification via column chromatography (eluent DCM/n-hexane 1:1.5 v/v, R_f 0.7), a white powder was obtained in 39 % yield; ^{1}H NMR ($CDCl_3$): δ 7.29 (s, 2H, O*H*), 7.10 (s, 4H, Ar*H*), 6.80 (s, 4H, Ar*H*), 4.31 (d, 4H, ^2J = 13.0 Hz, ArCH_2Ar), 3.98 (d, 6H, ^1J = 144.4 Hz, $^{13}CH_3$), 3.36 (d, 4H, ^2J = 13.0 Hz, ArCH_2Ar), 1.33 (s, 18H, t-C$_4H_9$), 0.97 (s, 18H, t-C$_4H_9$); ^{13}C NMR($CDCl_3$): δ 151.19, 150.51, 146.86, 141.53, 132.32, 127.90, 125.56, 125.09, 63.52, 60.88, 33.94, 33.88, 31.75, 31.42, 31.04; HR ESI MS calcd for $^{12}C_{44}^{13}C_2H_{60}O_4Na_1$ 701.4451, found 701.4444.

5,11,17,23-tetra-*tert*-butyl-25, 27-dipentyloxy-26, 28-dihydroxy-calix[4]arene (di-C_5). After purification via column chromatography (eluent DCM/n-hexane 1:1.5 v/v, R_f 0.8), a white powder was obtained in 56 % yield; ^{1}H NMR ($CDCl_3$): δ 7.89 (s, 2H, O*H*), 7.12 (s, 4H, Ar*H*), 6.92 (s, 4H, Ar*H*), 4.39 (d, 4H, ^2J = 12.8 Hz, ArCH_2Ar), 4.05 (t, 4H, ^3J = 6.8 Hz, OCH_2), 3.39 (d, 4H, ^2J = 12.8 Hz, ArCH_2Ar), 2.11 (m, 4H, CH_2), 1.74 (m, 4H, CH_2), 1.56 (m, 4H, CH_2), 1.36 (s, 18H, t-C$_4H_9$), 1.08 (s, 18H, t-C$_4H_9$), 1.07 (t, 6H, ^3J = 7.2 Hz, CH_3); ^{13}C NMR($CDCl_3$): δ 150.93, 150.13, 146.68, 141.25, 132.90, 127.87, 125.50, 125.09, 76.60, 34.02, 33.86, 31.91, 31.78, 31.15, 29.79, 28.25, 22.63, 14.21; HR ESI MS calcd for $^{12}C_{54}H_{76}O_4Na_1$ 811.5636, found 811.5633.

2.3.2 General Procedure for Synthesis Ti–Calixarene (Titanocalixarene) Complexes

Complexes mono-C_1-Ti, mono-C_5-Ti, di-C_1-Ti, and di-C_5-Ti were synthesized by adding to 0.9 equiv of $TiCl_4$ (1.0 M solution in toluene, Aldrich) to a 0.04 M solution of the corresponding calixarene ligand in toluene and stirring at 313 K for 1.5 h. Ti precursor was used as a limiting reagent to prevent formation of polymeric Ti species.

2.3.2.1 di-C_1-Ti After evaporation of solvent and dissolution in C_6D_6, ^{1}H NMR (C_6D_6) δ 7.17 (s, 4 H, Ar*H*), 6.82 (s, 4 H, Ar*H*), 4.60 (d, 4 H, $^2J_{HH}$ = 13.4 Hz, CH_2), 4.19 (d, 6 H, OCH_3, $^1J_{C,H}$ = 146 Hz), 3.19 (d, 4 H, $^2J_{HH}$ = 13.6 Hz, CH_2), 1.38 (s, 18 H, C(CH_3)$_3$), 0.68 (s, 18 H, C(CH_3)$_3$),^{13}C NMR (C_6D_6) δ 70.9 (OCH_3) observed due to ^{13}C enrichment at OCH_3 position. In agreement with literature [24].

2.3.2.2 di-C_5-Ti After evaporation of solvent and dissolution in C_6D_6, ^{1}H NMR (C_6D_6) δ 7.12 (s, 4 H, Ar*H*), 6.89 (s, 4 H, Ar*H*), 4.60 (d, 4 H, $^2J_{HH}$ = 13.4 Hz, CH_2), 5.04 (tt, 4 H, OCH_2-), 4.87 (d, 4H, CH_2, $^2J_{HH}$ = 13.2 Hz), 3.24 (d, 4 H, $^2J_{HH}$ = 13.6 Hz, CH_2), 2.03 (tt, 4 H, CH_2 alkyl), 1.42 (s, 18 H, C(CH_3)$_3$), 1.01 (tt, 4 H, CH_2 alkyl), 0.70 (m, 28 H, C(CH_3)$_3$ and CH_2CH_3 alkyl).

2.3.2.3 mono-C_1-Ti After evaporation of solvent and dissolution in C_6D_6, ^{1}H NMR (C_6D_6): δ 7.14 (s, 4 H, Ar*H*), 6.82 (s, 2 H, Ar*H*), 6.78 (s, 2 H, Ar*H*), 4.97 (d, $^2J_{H,H}$ = 12.8 Hz, 2 H, CH_2), 4.31 (d, $^2J_{H,H}$ = 12.8 Hz, 2 H, CH_2), 3.84 (d, 3 H, OCH_3, $^1J_{C,H}$ = 146 Hz), 3.22 (d, $^2J_{H,H}$ = 12.8 Hz, 2 H, CH_2), 3.13 (d, $^2J_{H,H}$ = 12.8 Hz, 2 H, CH_2), 1.37 [s, 18 H, C(CH_3)$_3$], 0.77 [s, 9 H, C(CH_3)$_3$], 0.68 [s, 9 H, C(CH_3)$_3$] ppm. ^{13}C NMR (C_6D_6): δ 65.4 (OCH_3) observed due to ^{13}C enrichment at OCH_3 position. In agreement with literature [22].

2.3.2.4 mono-C_5-Ti After evaporation of solvent and dissolution in C_6D_6, ^{1}H NMR (C_6D_6) δ aromatics overlap with residual toluene solvent, 5.03 (d, 2 H, $^2J_{HH}$ = 12.8 Hz, CH_2), 4.58 (d, 2 H, $^2J_{HH}$ = 12.4 Hz, CH_2), 4.48 (t, 2H, $^2J_{HH}$ = 6.4 Hz, OCH_2-alkyl), 3.33 (d, 2H, $^2J_{HH}$ = 13.2 Hz, CH_2), 3.29 (d, 2H, $^2J_{HH}$ = 12.6 Hz, CH_2), 1.94 (tt, 2 H, CH_2 alkyl), 1.48 (s, 18 H, C(CH_3)$_3$), 0.91 (m, 2 H, CH_2 alkyl), 0.82 (m, 23 H, C(CH_3)$_3$ and CH_2CH_3 alkyl).

2.3.3 General Procedure for Grafting of Ti–Calixarene Complexes onto SiO_2

Selecto Scientific Silica Gel SiO_2 (32–63 particle size) was treated under dry air and Ar for 4 h at 473 and 1073 K to prepare SiO_2@200 and SiO_2@800 supports, respectively, and transferred to an Ar glovebox under air-free conditions. 1 g of SiO_2 support was degassed under vacuum at 473 K for 2 h, cooled, and suspended in 10 mL of toluene. To this, 4 mL of the dissolved titanocalixarene complex was added, and stirred at room temperature for 18 h. The solids were decanted, the supernatant removed, and the solids washed with 5 × 40 mL of anhydrous toluene by subsequent decantation and supernatant removals, until the supernatant was colorless indicating all excess complex had been removed. The materials were dried under dynamic vacuum at 393 K for 1 h and stored in an Ar glovebox.

2.4 Catalysis

1-octene epoxidation rates and selectivity were measured by combining, in a 25 mL Schlenk flask, ~30 mg of catalyst (weighed under Ar) and ~300 mg of 4A molecular sieves (previously dehydrated at 573 K for 6 h) and treating the contents under dynamic vacuum at 393 K for 1 h. To this, 20 mL of a 0.18 M solution of 1-octene (distilled from CaH_2) in octane (distilled from sodium/benzophenone) were added, and the contents equilibrated under stirring to 323 K for 0.5 h. The reaction was started by addition of 0.125 mL of a 6.5 M solution of TBHP in nonane (Aldrich, concentration measured by iodometric

titration [30]), and aliquots were removed every 1 h and analyzed by gas chromatography using an Agilent 6890A gas chromatograph. As discussed elsewhere [15], epoxidation rates are proportional to catalyst, alkene, and oxidant concentrations:

$$\text{rate} = \frac{d[\text{TBHP}]}{dt} = k[\text{Ti}][\text{alkene}][\text{TBHP}] \quad (1)$$

where quantities in square brackets [] represent concentration in the reactor in mol/L. Selectivity was calculated based on the limiting reagent, TBHP, and is a measure of the efficiency with which oxidant consumption produces the desired epoxide product. It was calculated as the ratio of epoxide yield to TBHP conversion, with yield given by the ratio of epoxide produced to TBHP initially present, and conversion given by the ratio of TBHP consumed to TBHP initially present. TBHP and epoxide present in the reaction mixture were quantified by comparing gas chromatograph peak areas in aliquots of the reaction mixture to peak areas of external references prepared with known concentration of TBHP and epoxide within the range observed in the reaction mixture. Initial turnover frequencies (TOF_0) were calculated by extrapolating the TOF measured at each data point to initial time using a second order polynomial fit. TOF at each time point were calculated as the ratio of epoxide produced per Ti site per time.

3 Results and Discussion

3.1 Physicochemical Characterization of Titanocalixarene Grafting on SiO_2

Three distinct synthetic handles control the Ti coordination environment of catalysts in Scheme 1: (i) the choice of calixarene ligand, which controls the surface complex symmetry and the oxygen–titanium dative interactions (see Scheme 1); (ii) the choice of alkyl ether (methoxy C_1 or pentoxy C_5) substituent on the lower-rim phenolic oxygen; and (iii) the choice of SiO_2 support pretreatment temperature, which controls hydroxyl group surface density (low in SiO_2@800, high in SiO_2@200).

The coordination environment and corresponding physicochemical characterization for each grafted titanocalixarene material is summarized in Table 1. All materials show successful grafting of the intact titanocalixarene complex onto the support, as indicated by a nearly ~1:1 calixarene to titanium ratio. Observed deviations from this 1:1 ratio are attributed to experimental uncertainty in elemental analysis due to the lower site loading compared to our previous work [15, 31].

Grafting resulted in submonolayer surface coverages of the titanocalixarene complex [15], which we attribute to grafting being performed at mild, room temperature conditions here as opposed to reflux conditions of prior work, as well as the higher degree of silica-support dehydroxylation for the SiO_2@800 used here [15, 16]. This implies that only the most reactive surface hydroxyl groups successfully form covalent attachment to the titanocalixarene at milder conditions, which were chosen to be gentle so as to avoid conversion of di-C_1-Ti and di-C_5-Ti to mono-C_1-Ti and mono-C_5-Ti through lower-rim alkyl ether bond cleavage, which occurs in solution at higher temperatures [17]. The SiO_2@200 support, which consist of a near-maximum surface hydroxyl group coverage (expected to be ~5 OH/nm^2), accommodates a higher grafted site density when compared to SiO_2@800, with only about 15 % of the maximum hydroxyl group surface coverage (expected to be ~0.7 –OH/nm^2) [32]. The higher abundance of potential hydroxyl grafting sites, and the higher surface acidity due to weak silanol acid sites on SiO_2@200 facilitates Ti–Cl bond cleavage to form the Ti–O–Si connectivity in grafted species.

Grafted mono-C_1-Ti-SiO_2 sites consist of pseudo-tetrahedral Ti with three bonds to calixarene and one bond to the silica surface [15] (Scheme 1), and are thus supposed to contain no Cl from synthesis. However, despite our best efforts to remove HCl byproduct by washing and drying during synthesis, some Cl remains, as evidenced by measurable Cl content shown in Table 1 for mono-C_1-Ti-SiO_2@800. This is presumably the result of Si-Cl bond formation and/or physisorbed HCl. We note that a maximum 4 Cl:Ti ratio would be possible from $TiCl_4$ if no HCl were removed during washing of the grafted material. Notwithstanding this background Cl content, which introduces some experimental uncertainty to the analysis below, we attempt to use Cl elemental analysis as data that informs as to the number of silica attachment points for the di-R-Ti complexes.

di-R-Ti complexes will lose a Cl ligand upon grafting but have yet a second labile Cl ligand coordinated to the Ti center. When grafting on a highly hydroxylated surface, we observe the Cl:Ti ratio of di-C_1-Ti-SiO_2@200 (2.0) to be similar to that of mono-C_1-Ti-SiO_2@800 (1.3) (the slightly higher Cl content on SiO_2@200 is attributable to the higher HCl adsorption capacity of the more polar hydroxyl-rich silica surface). The similarity of Cl:Ti ratio between di-C_1-Ti-SiO_2@200 (2.0) and mono-C_1-Ti-SiO_2@800 (1.3) is consistent with bipodal attachment of di-C_1-Ti to adjacent silanols, as shown in Scheme 1, in agreement with previous demonstrations of bipodal grafting of Ti precursors with labile ligands onto SiO_2 at full surface hydroxyl coverages [14]. In contrast, the Cl:Ti ratio for the case of di-C_1-Ti-SiO_2@800 (3.2) increases by ~1 Cl when compared to di-

Table 1 Physicochemical and spectroscopic data for grafted materials

Material[a]	Coordination environment			Site density (nm^{-2})[b]		Calix:Ti ratio	Cl[e]:Ti ratio	LMCT edge energy (eV)
	Oxygen dative interaction	Support	O–R substituent	Calix[c]	Ti[d]			
di-C_1-Ti-SiO_2@800	di	SiO_2@800	O–CH_3	0.067	0.073	0.91	3.2	2.16[f]
mono-C_1-Ti-SiO_2@800	mono	SiO_2@800	O–CH_3	0.068	0.079	0.86	1.3	2.26[f]
di-C_1-Ti-SiO_2@200	di	SiO_2@200	O–CH_3	0.113	0.098	1.15	2.0	2.18
mono-C_1-Ti-SiO_2@200	mono	SiO_2@200	O–CH_3	0.098	0.092	1.07	–	2.23
di-C_5-Ti-SiO_2@800	di	SiO_2@800	O–$(CH_2)_4CH_3$	0.059	0.079	0.75	–	2.14
mono-C_5-Ti-SiO_2@800	mono	SiO_2@800	O–$(CH_2)_4CH_3$	0.083	0.098	0.85	–	2.24

[a] Labeled as on Scheme 1

[b] Based on a measured BET surface area of 402 m^2/g

[c] Based on combustion analysis

[d] Based on ICP-AES

[e] Cl content based on suppressed ion chromatography. Handled under air-free conditions to prevent Ti–Cl hydrolysis

[f] Measured at ±0.01 eV

C_1-Ti-SiO_2@200 (2.0). This is consistent with monopodal bonding of di-C_1-Ti to the SiO_2@800 surface and retention of a Ti–Cl bond as hypothesized in Scheme 1 for di-C_1-Ti-SiO_2@800. Under catalytic conditions, this Ti–Cl bond would presumably be converted to –OR (R = oxidant fragment *O-tert*-butyl or R = alcohol fragment *tert*-butyl) ligand.

Further confirmation of intact grafting of mono-C_1-Ti and di-C_1-Ti complexes comes from solid-state ^{13}C MAS NMR spectroscopy. For this, we synthesized ^{13}C isotopically enriched versions of mono-C_1 and di-C_1 ligands, at the methoxy lower-rim substituent (denoted R in Scheme 1). Enrichment at this position is evidenced by ^1H solution-phase NMR spectroscopy, showing a doublet for O-CH_3 with very strong coupling (^1J = 144–145 Hz), due to direct coupling with the ^{13}C nucleus. In contrast, a singlet is observed at this position for a regular ^{12}C nucleus due to the absence of coupling [22], [24]. As shown in Fig. 1a, the ^{13}C MAS NMR spectrum of mono-C_1-Ti-SiO_2@800 exhibits a single broad resonance centered about 64 ppm, which is near the 65 ppm resonance of the mono-C_1-Ti complex in solution. The principal ^{13}C MAS NMR resonance for di-C_1-Ti-SiO_2@800 is centered about 69 ppm in Fig. 1b, again at slightly higher field from the 71 ppm observed in solution for di-C_1-Ti. Upon integrating the total area under the methoxy resonance, a 1.9-fold higher integrated area per Ti is observed for di-C_1-Ti-SiO_2@800 relative to mono-C_1-Ti-SiO_2@800 (Supplementary Figure 1; Table 1). This ratio being so nearly equal to 2.0 suggests that both methoxy substituents on the di-C_1-Ti-SiO_2@800 precursor survive our gentle grafting conditions, and further support the structures shown in Scheme 1.

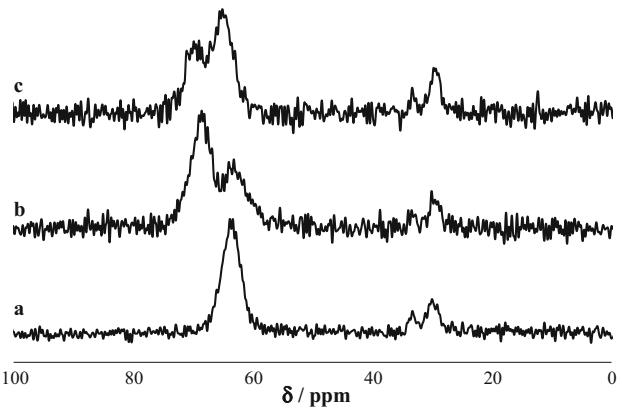

Fig. 1 ^{13}C MAS solid-state NMR spectrum of **a** mono-C_1-Ti-SiO_2@800, **b** di-C_1-Ti-SiO_2@800, **c** di-C_1-Ti-SiO_2@200. The strongest resonances correspond to ^{13}C labeled methoxy lower-rim substituents. Resonances between 20–40 ppm arise due to upper-rim *tert*-butyl substituents, which are not isotopically enriched

In solution-phase ^{13}C NMR spectroscopy (see "Experimental" Section), a downfield shift of ~6 ppm in the principal methoxy resonance of di-C_1-Ti is observed when compared to mono-C_1-Ti, which we attribute to stronger methoxy coordination to the Ti center in di-C_1-Ti. In addition, the ^1H chemical shift of mono-C_1-Ti O–CH_3 resonance is 3.84 ppm, in contrast to di-C_1-Ti O–CH_3 resonance at 4.18 ppm. The same result is independent of alkoxy substituent, as mono-C_5-Ti and di-C_5-Ti also exhibit this effect, with di-C_5-Ti O–CH_2–resonances at 5.05 ppm while mono-C_5-Ti O–CH_2–are at 4.48 ppm. Such deshielded alkoxy ether resonances for the di-R-Ti complexes are indicative of stronger dative bonding and

shorter Ti–OCH_3 bond distances in the di-R-Ti complex relative to mono-R-Ti, consistent with previously reported single-crystal X-ray diffraction data, in which Ti–OCH_3 bond distances were measured for mono-C_1-Ti and di-C_1-Ti at 2.4 [22] and 2.1 Å [24], respectively. These distances suggest stronger dative methoxy coordination to the Ti Lewis acid site in di-C_1-Ti compared to mono-C_1-Ti and support the observed downfield shift in the grafted sites described above. This effect of stronger coordination due to shorter RO–Ti distances was previously predicted by us based on simple geometric models using both data from electronic-structure calculations and single-crystal X-ray diffraction. We further hypothesized that this stronger RO–Ti interaction would lead to higher 3d-orbital occupancy at the Ti center [20], which in turn was predicted to lead to suppressed catalytic activity, based on previous studies correlating higher 3d-orbital occupancy to decreases activity for olefin epoxidation [17].

It is important to note the information about titanocalixarene complex symmetry from ^1H solution-phase NMR spectroscopy of the precursor complexes (see "Experimental" Section). Both di-C_1-Ti and di-C_5-Ti present only two distinct CH_2 methylene bridge resonances in the calixarene, while mono-C_1-Ti and mono-C_5-Ti present four distinct resonances at this position, indicating the expected different symmetry of coordination (C_{2v} in di-R-Ti [24] vs. C_s for mono-R-Ti [22]). Similarly, only one resonance is observed in ^{13}C solution-phase NMR at the –OCH_3 position because only one such carbon is present in mono-C_1-Ti and because of C_{2v} symmetry in di-C_1-Ti. These symmetry assignments further support the reasoning in the paragraph above. However, unlike the solution-phase ^{13}C NMR spectrum of di-C_1-Ti, the ^{13}C solid-state NMR spectrum for di-C_1-Ti-SiO_2@800 and for di-C_1-Ti-SiO2@200 exhibits a second upfield resonance centered around 63–65 ppm, as shown in Fig. 1b, c. This second resonance indicates an additional chemical environment surrounding Ti centers in di-C_1-Ti-SiO_2, which is not present in solution, and which may arise from the heterogeneity inherent in the silica surface. This heterogeneity presumably leads to the flexible calixarene ligand adopting a different conformation in the grafted form of the complex, different from that in solution.

Previous elegant studies by Radius [24], have analyzed the different conformations that the di-C_1-Ti complex can adopt via molecular modeling. While the most energetically favorable conformation corresponds to both methoxy substituents being "exo", the second lowest energy contributor involves a conformation in which one of the methoxy substituents is "endo", as represented in Scheme 1. This "endo" conformation results in Ti–OCH_3 distances of 2.4–2.5 Å (Supplementary Figure 2, LiTiCl2_"endo"), significantly longer than for the "exo" conformation (2.1 Å [24]) and similar to distances in mono-C_1-Ti (2.4 Å [22]). The similarity of the measured bond distances between mono-C_1-Ti and those calculated for the "endo" conformation of the di-C_1-Ti suggests a similar chemical shift for methoxy resonances. This is consistent with the observed similarity of the chemical shifts for the shoulder resonance described above (63–65 ppm) and the methoxy resonance of mono-C_1-Ti-SiO_2@800 (64 ppm), suggesting that the upfield resonance in grafted di-C_1-Ti may correspond to the "endo" conformer of di-C_1-Ti-SiO_2. While this conformation is energetically less favored according to calculations [24], and is not detected in solution for di-C_1-Ti, it presumably becomes favorable in the grafted complexes due to the impinging proximity of the heterogeneous silica surface in a certain fraction of sites. Further evidence for the existence of the "endo" conformation is seen when comparing Figs. 1b and 1c of the same complex, di-C_1-Ti, on supports of different hydroxyl density, SiO_2@800 and SiO_2@200, respectively. On SiO_2@200, the upfield "endo" resonance becomes more prominent (64 % of integrated area on SiO_2@200, only 31 % on SiO_2@800, Supplementary Table 2) than the "exo" resonance, implying that di-C_1-Ti is grafts predominantly as the "endo" conformer. This is consistent with the conformational change from "exo" to "endo" being induced by the proximity of the SiO_2 surface, which is presumably closer to the calixarene ligands for complexes grafted on SiO_2@200 due to the bipodal attachment of di-C_1-Ti, as opposed to monopodal attachment on SiO_2@800, as outlined above. We further expect that upon adsorption of the oxidant during catalysis, steric crowding may lead to more grafted sites being in the "endo" conformation.

Altogether, these results cumulatively suggest that the materials prepared display at least three molecularly distinct active sites with different Ti coordination environments, as summarized in Scheme 1: tripodal connectivity to the calixarene with monopodal attachment to the silica surface (all mono-R ligand materials), dipodal attachment to both the calixarene and the silica surface (di-C_1-Ti-SiO_2@200), and dipodal attachment to calixarene with monopodal attachment to the silica surface and a free (-Cl) coordination site (di-R-Ti-SiO_2@800), with both "endo" and "exo" conformers for the latter two.

3.2 Spectroscopic Comparison of the Ti Coordination Environment in Grafted Materials

Further evidence of differing electronic environments in di-R-Ti compared to the mono-R-Ti grafted complexes comes from diffuse reflectance UV–visible spectra and calculated LMCT edge energies. As shown in Fig. 2, all materials display the absorption centered at 230 nm that is indicative

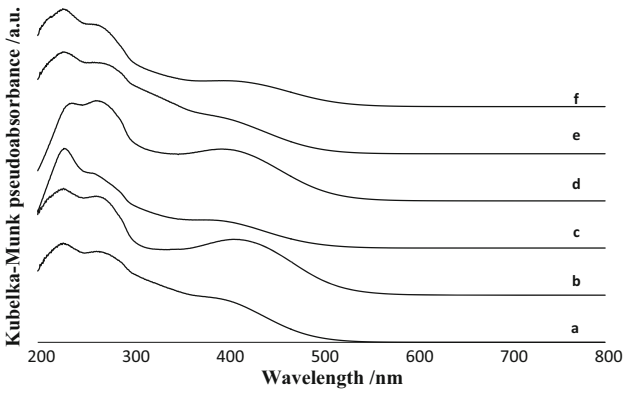

Fig. 2 Diffuse reflectance UV–visible spectra for all grafted materials. **a** mono-C_1-Ti-SiO_2@800, **b** di-C_1-Ti-SiO_2@800, **c** mono-C_1-Ti-SiO_2@200, **d** di-C_1-Ti-SiO_2@200, **e** mono-C_5-Ti-SiO_2@800, **f** di-C_1-Ti-SiO_2@800

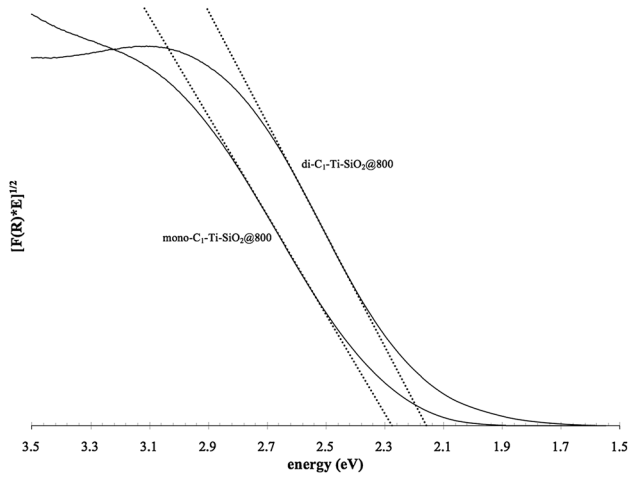

Fig. 3 Diffuse-reflectance UV–visible spectra of representative grafted complexes mono-C_1-Ti-SiO_2@800 and di-C_1-Ti-SiO_2@800. Both spectra use the Kubelka–Munk formalism (denoted as F(R)) and assume indirect LMCT transitions. LMCT edge energies are defined as the intercept of the shown (*dotted*) *tangent lines* calculated from the 1st derivative of the transformed spectra. E denotes energy

isolated Ti sites [33], a 270–290 nm band arising from π–π* aromatic transitions, and a broad absorption feature at 290–500 nm, previously assigned to Ti(IV)-calixarene charge transfer (LMCT) transitions [15]. A higher intensity of this latter band in materials with di-R calixarene ligands is observed and is independent of the SiO_2 support used (traces b and d in Fig. 2). This is visually apparent due to a strong, opaque, red coloring of di-R-Ti complexes in solution compared to the more translucid, lighter red coloring of mono-R-Ti complexes, a visible difference which persists in the grafted materials.

All mono-R-Ti-SiO_2 complexes have LMCT edge energies at 2.24 ± 0.02 eV, in agreement with previous work [16]. No influence of lower-rim alkyl-ether substituent is observed, as indicated by similar LMCT energies for mono-C_1-Ti-SiO_2@800 and mono-C_5-Ti-SiO_2@800 as well as di-C_1-Ti-SiO_2@800 and di-C_5-Ti-SiO_2@800. However, a decrease in LMCT energy to 2.16 ± 0.02 eV for di-R-Ti@SiO_2 materials is observed, as illustrated by differing intercepts for selected materials in Fig. 3. Previous studies have demonstrated that LMCT energies are insensitive to a large number of substituents on the calixarene upper-rim [16, 34] and even strong oxygen coordination to the Ti center [17]. This leads us to conclude that the different coordination geometry surrounding the Ti center is responsible for the variation in LMCT energy. Extended Hückel calculations of the two geometries have shown that geometry does affect the energetics of frontier orbitals responsible for LMCT transitions [35] and lowers Ti LUMO by ∼0.1 eV in di-C_1-Ti when compared to mono-C_1-Ti [23], consistent with the measured differences in LMCT edge energies in these materials.

The LMCT edge energies provide a useful fingerprint that differentiates mono-R-Ti and di-R-Ti grafted surface complexes. Combined with previous physicochemical characterization demonstrating unique coordination to Ti, these materials provide a well-defined molecular system to test the influence of ligand coordination to Ti on catalytic activity.

3.3 Catalysis

All titanocalixarene materials prepared are active catalysts for the epoxidation of 1-octene in octane at 323 K using *tert*-butyl hydroperoxide (TBHP) as the oxidant, as summarized in Table 2. The catalytic activity of different materials was used as a probe for the influence of the Ti coordination environment on catalysis. Catalytic activity was compared in terms of (i) TOF extrapolated to initial time using a second order polynomial fit, as shown in Fig. 4; (ii) a pseudo 1st order rate for TBHP decomposition, as shown in Supplementary Figure 3; (iii) selectivity at ∼30 % conversion, defined as the ratio of epoxide produced to oxidant consumed. These values of initial TOF at 50 °C are similar to those previously observed for titanocalixarene materials for this reaction [31], and are indicative of persistent grafting of titanocalixarene complexes onto SiO_2, since homogeneous titanocalixarenes from potentially leached sites have been demonstrated to be inactive for epoxidation [15], [16]. We performed a hot filtration experiment [36], in which the solid catalyst was filtered out of solution at catalytic conditions and epoxidation activity ceased, in order to confirm that surface grafted di-R-Ti complexes do not leach into solution as active catalysts (Supplementary Figure 4). The results of this indicate that novel grafted di-R-Ti-SiO_2 catalysts described in this work are truly heterogeneous in nature

Table 2 Epoxidation rates and selectivities for different grafted titanocalixarene sites

Material	Coordination environment			Temp. (°C)	k_{TBHP} (M^{-2} s^{-1})[a]	TOF_0 (ks^{-1})[b]	Selectivity[c]
	Oxygen dative interaction	Support	O–R substituent				
di-C_1-Ti-SiO_2@800	di	SiO_2@800	O–CH_3	50	1.6	4.4	0.43
				65	4.4	15	0.47
				80	5.5	24	0.47
Mono-C_1-Ti-SiO_2@800	mono	SiO_2@800	O–CH_3	50	1.5	4.2	0.43
				65	4.0	10	0.38
				80	5.5	20	0.39
di-C_1-Ti-SiO_2@200	di	SiO_2@200	O–CH_3	50	0.98	2.0	0.40
Mono-C_1-Ti-SiO_2@200	mono	SiO_2@200	O–CH_3	50	0.97	2.2	0.43
di-C_5-Ti-SiO_2@800	di	SiO_2@800	O–$(CH_2)_4CH_3$	50	1.7	4.2	0.43
mono-C_5-Ti-SiO_2@800	mono	SiO_2@800	O–$(CH_2)_4CH_3$	50	1.5	3.2	0.40

[a] Pseudo 1st order rate constant based on the consumption of TBHP. Reaction was carried out in excess olefin (<3 % olefin conversion at 30–40 % TBHP conversion)

[b] Initial turnover frequency, defined as amount of epoxide produced per Ti site per time (measured in kiloseconds), extrapolated to initial time

[c] Ratio of epoxide yield with respect to initial TBHP present to TBHP conversion after 6 h of reaction. ~30 % conversion at 50 °C, ~75 % conversion at 65 °C, ~85% conversion at 80 °C

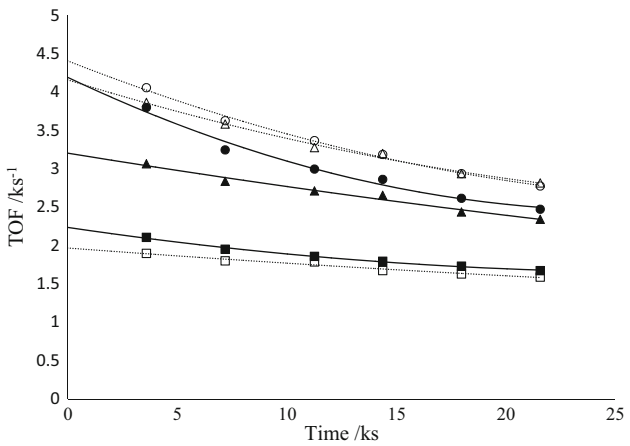

Fig. 4 Catalytic turnover frequency (TOF) as a function of time for grafted titanocalixarene catalysts. 2nd order polynomial fits used for extrapolation are shown. mono-C_1-Ti-SiO_2@800 (*filled circle*, *solid line*), di-C_1-Ti-SiO_2@800 (*unfilled circle*, *dotted line*), mono-C_5-Ti-SiO_2@800 (*filled triangle*, *solid line*), di-C_5-Ti-SiO_2@800 (*unfilled triangle*, *dotted line*), mono-C_1-Ti-SiO_2@200 (*filled square*, *solid line*), di-C_1-Ti-SiO_2@200 (*unfilled square*, *dotted line*)

just as their previously described mono-R-Ti-SiO_2 analogues [15].

Materials supported on SiO_2@200 showed ~40 % slower rates of consumption of TBHP for both mono-C_1-Ti and di-C_1-Ti grafted complexes. Given that the decrease is similar for both complexes, we can exclude the possibility that bipodal attachment to silica in di-C_1-Ti-SiO_2@200 when compared to di-C_1-Ti-SiO_2@800 is responsible for decreased activity, since mono-C_1-Ti grafts through a single Ti–OSi in both SiO_2 supports. This leads us to conclude that the outer-sphere slightly affects TBHP consumption rates.

At these conditions, all materials reached ~30 to 40 % conversion of TBHP and <3 % conversion of 1-octene at 50 °C after 6 h with 40–43 % selectivity, indicating that 40–43 % of TBHP is consumed towards epoxide formation as opposed to unproductive decomposition to *tert*-butyl alcohol (TBOH). Along with TBHP consumption, a concomitant increase in TBOH in solution was observed, but no significant olefin oxidation byproducts were detected. This low selectivity has been previously attributed to the relative difficulty of epoxidation for terminal alkenes such as 1-octene [15].

When comparing grafted mono-R-Ti to di-R-Ti complexes on the same support and with the same lower-rim alkyl ether substituent, rate constants are within 13 % of each other for all temperatures (Table 2). This indicates that the catalytic activity is virtually unaffected by the inner-coordination sphere for Ti as enforced by the calixarene ligand. This outcome is an unexpected and surprising result given the stronger dative coordination expected and observed by NMR spectroscopy in di-R-Ti relative to mono-R-Ti in the resting state (i.e. prior to catalytic testing), as well as the previously observed correlation between decreased Lewis acidity and epoxidation activity with increased dative coordination [17].

One possible interpretation for this unexpected outcome, consistent with these and all previous results, is that the grafted di-R-Ti site undergoes a further conformational change to the "endo" conformer (Scheme 1) under

catalysis conditions. Indeed, the di-R calixarene ligands used here are prone to undergoing conformational changes given the symmetric dipodal attachment of Ti to the calixarene and the known flexibility of calixarenes [37]. While ^{13}C solid-state NMR spectroscopy showed only 31 % of sites in di-C_1-Ti-SiO_2@800 and 64 % of sites in di-C_1-Ti-SiO_2@200 were in the "endo" conformation in the catalyst "resting state" (Sup. Table 2), the flexibility of the calixarene means that under catalytic conditions, where bulky TBHP is expected to be bound to the Ti center [16], more sites may adopt this conformation, similar to the observed trend favoring the "endo" conformer when comparing di-C_1-Ti-SiO_2@200 and -SiO_2@800 (see Section 3.1). This "endo" conformation, with longer RO–Ti distances, is expected to have a similar 3d-electron occupancy to grafted mono-C_1-Ti sites and thus a similar catalytic activity, which could explain the small differences in initial TOF and k_{TBHP} when comparing grafted mono-R-Ti to di-R-Ti sites.

The prevalence of the "endo" conformation during catalysis would lead to a Ti center that is spatially less constrained and more accessible to attack by the oxidant and olefin than a grafted Ti center where the calixarene remains in its "exo" cone conformation. The high degree of accessibility of grafted titanocalixarene centers to a bulky oxidant such as TBHP is indeed surprising, given the steric bulk of spatial constraints imposed by a surrounding calixarene macrocycle. Previously, it has been proposed, based on kinetic and thermodynamic arguments, that either (calix)Ti–O(SiO_2) or (calix)–TiO(SiO_2) cleave during the kinetically relevant step [15, 17], providing accessibility for adsorption of TBHP onto Ti. Here, the observation of an "endo" calixarene conformer suggests that a conformational change of the calixarene ligand could lead to sterically accessible Ti centers in all grafted titanocalixarene catalysts.

There is one additional possibility, besides a predominant "endo" conformation during catalysis, that may account for the observed similarity of rates between grafted mono-R-Ti and di-R-Ti sites, which is discussed below. Recovery of di-C_1-Ti-SiO_2 catalysts isotopically enriched at the methoxy ether position used for epoxidation and subsequent MAS ^{13}C solid-state NMR spectroscopy showed only a single, broad, upfield resonance at 63–65 ppm when compared to materials in the resting state (see Supplementary Figure 5). While this shift is consistent with the "endo" conformer prevailing after catalysis due to TBHP coordination inducing a conformational change, a 40–50 % decrease in methoxy resonance, without concomitant loss of calixarene ligand, is observed (see Supplementary Table 2). The similarity in chemical shift of this upfield resonance to the chemical shift of grafted mono-C_1-Ti suggests that it is possible that after catalyst recovery, cleavage of the methoxy ether may result in the transformation of di-C_1-Ti into mono-C_1-Ti. While this transformation is known to occur in solution through lower-rim alkyl ether bond cleavage [17], it is unexpected for surface grafted species which were stable upon drying at 393 K, which is a higher temperature than that used in catalysis (333 K). This transformation would imply that two catalysts with different inner coordination environments in the resting state may adopt a similar coordination environment in the active state, and thus display similar epoxidation activities as observed here. It is important to note, however, that catalyst recovery involved reaction under deactivating conditions (without molecular sieves), washing, drying, and storage (see Supplementary Figure 5) which are not representative of the state of the calixarene ligand under reaction conditions and add uncertainty to this analysis. In-situ ^{13}C MAS solid-state NMR spectroscopy experiments would be needed in the future to asses the state of the calixarene ligand under reaction conditions.

Studies for mono-C_1-Ti-SiO_2@800 and di-C_1-Ti-SiO_2@800 were extended to higher temperatures and demonstrate differences in selectivity between the two symmetries, as shown in Fig. 5. This observation argues for a lack of methoxy cleavage under catalysis conditions, which cannot be decisively ruled out given the discussion above. Catalyst di-C_1-Ti-SiO_2@800 is consistently more selective than mono-C_1-Ti-SiO_2@800 despite rate constants (Table 2, maximum 13 % difference at a given temperature) and activation energies (Supplementary Figure 6, 11 % difference) for TBHP consumption at all temperatures being almost indistinguishable between the two symmetries. Altogether, this data illustrates the

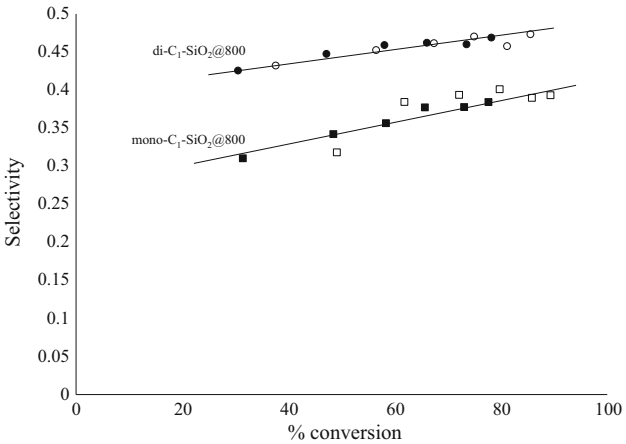

Fig. 5 Plot of conversion versus selectivity of TBHP towards epoxide, showing scatter in the results but an overall increase of selectivity with conversion, and better selectivity of grafted di-C_1-Ti when compared to mono-C_1-Ti materials at higher temperatures. Lines shown are interned as a guide to the eye. Each data point corresponds to a different time point during the reaction

importance of tuning the inner-sphere Ti coordination environment in epoxidation catalysis.

4 Conclusions

In this study, we have sought to gain a greater understanding of the influence that the organic ligand coordination sphere surrounding a grafted Ti cation has on its catalytic activity. We investigated this question by enforcing different Ti coordination environments using calixarene ligands, providing unique synthetic controls to prepare uniform, well-defined catalytic sites, and probed how this environment affects epoxidation activity, when using an organic hydroperoxide as the oxidant.

The symmetry of the Ti site, as enforced by grafting either a mono-R-Ti (C_s symmetry) or a di-R-Ti (C_{2v} symmetry) complex, is found to have significant effects on the nature of the grafted site. ^{13}C MAS NMR spectroscopy demonstrates the same single methoxy resonance for grafted mono-C_1-Ti as the complex in solution, indicating intact titanocalixarene grafting. The upfield resonance of the methoxy carbon in mono-C_1-Ti-SiO_2@800 (64 ppm) when compared to di-C_1-Ti-SiO_2@800 (69 ppm) indicates stronger electronic deshielding at the methoxy position, confirming our hypothesis that RO→Ti dative interactions are stronger in the grafted di-C_1-Ti complex due to shorter RO–Ti distances. LMCT edge energies of 2.24 ± 0.02 eV for mono-R-Ti@SiO_2 and 2.16 ± 0.02 eV for di-R-Ti@SiO_2 materials show differences in the electronic properties of the Ti center as enforced by the coordination geometry of the organic ligand, in the catalyst resting state. However, the ^{13}C MAS NMR spectrum of di-C_1-Ti-SiO_2@800 and di-C_1-Ti-SiO_2@200 also shows an upfield-shifted shoulder resonance, which we attribute to an unexpected "endo" conformer of the grafted complex. This "endo" conformer, brought about by the steric constraints of the impinging SiO_2 surface, has longer Ti–OR distances (i.e. weaker dative interactions) than the "exo" conformer according to prior molecular modeling studies—something that is consistent with its observed upfield shift.

We had previously hypothesized that stronger RO→Ti dative interactions in grafted di-R-Ti complexes would lead to lower Lewis acidity of Ti and lower epoxidation rates [20]; however, in this work, epoxidation activity as measured by rates of TBHP consumption is found to be largely unaffected by the symmetry of the grafted titanocalixarene. We thus propose two hypotheses: (a) under catalytic conditions, in the working state, grafted di-R-Ti sites exist in their "endo" conformation, which exhibits a similar RO–Ti distance and predicted 3d-electron occupancy based on this distance as mono-R-Ti; (b) that under catalytic conditions di-R-Ti undergoes a rearrangement to mono-R-Ti. Both possibilities are consistent with the similar rates of epoxidation observed and illustrate the need to assess the state of grafted organometallic catalytic sites in the active state, as they may, when grafted on a surface, exhibit additional complexities not seen in solution. The observation of an "endo" conformer in the catalyst resting state, which may prevail during catalysis, may more generally help elucidate a mechanism for accessibility in all grafted titanocalixarene catalysts. Namely, the switch from "exo" to "endo" conformation could be key in transforming a sterically crowded grafted titanocalixarene center to one that is more open for the binding of substrates involved in the kinetically relevant step for epoxidation. Despite these limited effects on TBHP consumption rates, measurable improvements in selectivity (45 vs. 34 % at a 50 % conversion) for di-C_1-Ti-SiO_2@800 when compared to mono-C_1-Ti-SiO_2@800 demonstrates the importance that coordination environment plays in determining catalytic activity, and illustrates the importance of precisely controlling the molecular environment of catalytic active sites in formulating the most effective catalyst.

Acknowledgments The authors are grateful to Prof. Dr. Udo Radius for providing structural data from previous molecular modeling studies [24] of Ti-calixarene complexes, and Dr. Kathleen Durkin for assistance with data analysis. Funding from the U.S. Department of Energy Office of Basic Energy Sciences (DE-FG02-05ER15696) and the National Science Foundation (IIP 1542974) is gratefully acknowledged.

References

1. Bell AT (2003) The impact of nanoscience on heterogeneous catalysis. Science 299:1688–1691. doi:10.1126/science.1083671
2. Copéret C, Chabanas M, Petroff Saint-Arroman R, Basset J-M (2003) Homogeneous and heterogeneous catalysis: bridging the gap through surface organometallic chemistry. Angew Chem Int Ed Engl 42:156–181. doi:10.1002/anie.200390072
3. Corma A, García H (2002) Lewis acids as catalysts in oxidation reactions: from homogeneous to heterogeneous systems. Chem Rev 102:3837–3892. doi:10.1021/cr010333u
4. Corma A (2004) Attempts to fill the gap between enzymatic, homogeneous, and heterogeneous catalysis. Catal Rev 46:369–417. doi:10.1081/CR-200036732
5. Dusi M, Mallat T, Baiker A (2000) Epoxidation of functionalized olefins over solid catalysts. Catal Rev 42:213–278. doi:10.1081/CR-100100262
6. Marchese L, Gianotti E, Dellarocca V et al (1999) Structure–functionality relationships of grafted Ti-MCM41 silicas. spectroscopic and catalytic studies. Phys Chem Chem Phys 1:585–592. doi:10.1039/a808225a
7. Thomas JM, Sankar G (2001) The role of synchrotron-based studies in the elucidation and design of active sites in titanium—silica epoxidation catalysts. Acc Chem Res 34:571–581. doi:10.1021/ar010003w
8. Corma A (2003) State of the art and future challenges of zeolites as catalysts. J Catal 216:298–312. doi:10.1016/S0021-9517(02)00132-X

9. Saxton RJ (1999) Crystalline microporous titanium silicates. Top Catal 9:43–57. doi:10.1023/A:1019102320274
10. Clerici M (1993) Epoxidation of lower olefins with hydrogen peroxide and titanium silicalite. J Catal 140:71–83. doi:10.1006/jcat.1993.1069
11. Maschmeyer T, Rey F, Sankar G, Thomas JM (1995) Heterogeneous catalysts obtained by grafting metallocene complexes onto mesoporous silica. Nature 378:159–162. doi:10.1038/378159a0
12. Guidotti M, Ravasio N, Psaro R et al (2003) Epoxidation on titanium-containing silicates: do structural features really affect the catalytic performance? J Catal 214:242–250. doi:10.1016/S0021-9517(02)00152-5
13. Jarupatrakorn J, Tilley TD (2002) Silica-supported, single-site titanium catalysts for olefin epoxidation. A molecular precursor strategy for control of catalyst structure. J Am Chem Soc 124:8380–8388. doi:10.1021/ja0202208
14. Bouh AO, Rice GL, Scott SL (1999) Mono- and dinuclear silica-supported titanium(IV) complexes and the effect of TioTi connectivity on reactivity. J Am Chem Soc 121:7201–7210. doi:10.1021/ja9829160
15. Notestein JM, Iglesia E, Katz A (2004) Grafted metallocalixarenes as single-site surface organometallic catalysts. J Am Chem Soc 126:16478–16486. doi:10.1021/ja0470259
16. Notestein JM, Solovyov A, Andrini LR et al (2007) The role of outer-sphere surface acidity in alkene epoxidation catalyzed by calixarene-Ti(IV) complexes. J Am Chem Soc 129:15585–15595. doi:10.1021/ja074614g
17. Notestein JM, Andrini LR, Kalchenko VI et al (2007) Structural assessment and catalytic consequences of the oxygen coordination environment in grafted Ti-calixarenes. J Am Chem Soc 129:1122–1131. doi:10.1021/ja065830c
18. Nandi P, Tang W, Okrut A et al (2013) Catalytic consequences of open and closed grafted Al(III)-calix[4]arene complexes for hydride and oxo transfer reactions. Proc Natl Acad Sci USA 110:2484–2489. doi:10.1073/pnas.1211158110
19. Nandi P, Solovyov A, Okrut A, Katz A (2014) Al III–Calix[4]-arene catalysts for asymmetric meerwein–ponndorf–verley reduction. ACS Catal 4:2492–2495. doi:10.1021/cs5001976
20. de Silva N, Hwang S-J, Durkin KA, Katz A (2009) Vanadocalixarenes on silica: requirements for permanent anchoring and electronic communication. Chem Mater 21:1852–1860. doi:10.1021/cm803392m
21. Trent DL (2000) Propylene oxide. In: Kirk-Othmer encyclopedia of chemical technology. Wiley, Hoboken
22. Friedrich A, Radius U (2004) A calix[4]arene monoalkyl ether as a model of a tris(phenolate) ligand with a hemilabile anisole moiety: syntheses, molecular structures and bonding of calix[4]arene ether supported titanium complexes and their catalytic activity in epoxidation reactions. Eur J Inorg Chem 2004:4300–4316. doi:10.1002/ejic.200400430
23. Zanotti-Gerosa A, Solari E, Giannini L et al (1998) Titanium-carbon functionalities on an oxo surface defined by a calix[4]arene moiety and its redox chemistry. Inorganica Chim Acta 270:298–311. doi:10.1016/S0020-1693(97)05863-5
24. Radius U (2001) Shaping the cavity of the macrocyclic ligand in metallocalix[4]arenes: the role of the ligand sphere. Inorg Chem 40:6637–6642. doi:10.1021/ic010482v
25. Böhmer V (1995) Calixarene—makrocyclen mit (fast) unbegrenzten möglichkeiten. Angew Chemie 107:785–818. doi:10.1002/ange.19951070704
26. Dijkstra PJ, Brunink JAJ, Bugge KE et al (1989) Kinetically stable complexes of alkali cations with rigidified calix[4]arenes: synthesis, X-ray structures, and complexation of calixcrowns and calixspherands. J Am Chem Soc 111:7567–7575. doi:10.1021/ja00201a045
27. Shang S, Khasnis DV, Burton JM et al (1994) From a novel silyl *p*-tert-Butylcalix[4]arene triether to mono-*O*-alkyl substitution: a unique, efficient, and selective route to mono-*O*-substituted calix[4]arenes. Organometallics 13:5157–5159. doi:10.1021/om00024a067
28. Groenen LC, Ruël BHM, Casnati A et al (1991) Synthesis of monoalkylated calix[4]arenes via direct alkylation. Tetrahedron 47:8379–8384. doi:10.1016/S0040-4020(01)96179-4
29. van Loon J-D, Verboom W, Reinhoudt DN (1992) Selective functionalization and conformational properties of calix[4]arenes, a review. Org Prep Proced Int 24:437–462. doi:10.1080/00304949209356227
30. Zawadiak J, Gilner D, Kulicki Z, Baj S (1993) Concurrent iodimetric determination of cumene hydroperoxide and dicumenyl peroxide used for reaction control in dicumenyl peroxide synthesis. Analyst 118:1081. doi:10.1039/an9931801081
31. Winner L, Daniloff G, Nichiporuk RV et al (2015) Patterned grafted lewis-acid sites on surfaces: olefin epoxidation catalysis using tetrameric Ti(IV)–calix[4]arene complexes. Top Catal 58:441–450. doi:10.1007/s11244-015-0385-x
32. Zhuravlev LT (1987) Concentration of hydroxyl groups on the surface of amorphous silicas. Langmuir 3:316–318. doi:10.1021/la00075a004
33. Marchese L, Maschmeyer T, Gianotti E et al (1997) probing the titanium sites in Ti–MCM41 by diffuse reflectance and photoluminescence UV–Vis spectroscopies. J Phys Chem B 101:8836–8838. doi:10.1021/jp971963w
34. Notestein JM, Iglesia E, Katz A (2007) Photoluminescence and charge-transfer complexes of calixarenes grafted on TiO 2 nanoparticles. Chem Mater 19:4998–5005. doi:10.1021/cm070779c
35. Fantacci S, Sgamellotti A, Re N, Floriani C (2001) Density functional study of tetraphenolate and calix[4]arene complexes of early transition metals. Inorg Chem 40:1544–1549. doi:10.1021/ic0004028
36. Prieto-Centurion D, Notestein JM (2011) Surface speciation and alkane oxidation with highly dispersed Fe(III) sites on silica. J Catal 279:103–110. doi:10.1016/j.jcat.2011.01.007
37. Böhmer V (1995) Calixarenes, macrocycles with(almost) unlimited possibilities. Angew Chemie 34:785–818. doi:10.1002/anie.199507131